

## Curcumin restores Nrf2 levels and prevents quinolinic acid-induced neurotoxicity<sup>☆</sup>

Iván Carmona-Ramírez<sup>a</sup>, Abel Santamaría<sup>b</sup>, Julio C. Tobón-Velasco<sup>b,c</sup>, Marisol Orozco-Ibarra<sup>d</sup>, Irma G. González-Herrera<sup>b</sup>, José Pedraza-Chaverri<sup>c</sup>, Perla D. Maldonado<sup>a,\*</sup>

<sup>a</sup>Patología Vascular Cerebral, Instituto Nacional de Neurología y Neurocirugía "Manuel Velasco Suárez", México D.F., 14269, México

<sup>b</sup>Aminoácidos Excitadores, Instituto Nacional de Neurología y Neurocirugía "Manuel Velasco Suárez", México D.F., 14269, México

<sup>c</sup>Departamento de Biología, Facultad de Química, Universidad Nacional Autónoma de México, México D.F., 04510, México

<sup>d</sup>Neurobiología Molecular y Celular, INNN-UNAM, Instituto Nacional de Neurología y Neurocirugía "Manuel Velasco Suárez", México D.F., 14269, México

Received 5 July 2011; received in revised form 13 December 2011; accepted 22 December 2011

### Abstract

Neurological diseases comprise a group of heterogeneous disorders characterized by progressive brain dysfunction and cell death. In the next years, these diseases are expected to constitute a world-wide health problem. Because excitotoxicity and oxidative stress are involved in neurodegenerative diseases, it becomes relevant to describe pharmacological therapies designed to activate endogenous cytoprotective systems. Activation of transcription factor Nrf2 stimulates cytoprotective vitagenes involved in antioxidant defense. In this work, we investigated the ability of the antioxidant curcumin to induce transcription factor Nrf2 in a neurodegenerative model induced by quinolinic acid in rats. Animals were administered with curcumin (400 mg/kg, p.o.) for 10 days, and then intrastriatally infused with quinolinic acid (240 nmol) on day 10 of treatment. Curcumin prevented rotation behavior (6 days post-lesion), striatal morphological alterations (7 days post-lesion) and neurodegeneration (1 and 3 days post-lesion) induced by quinolinic acid. Curcumin also reduced quinolinic acid-induced oxidative stress (measured as protein carbonyl content) at 6 h post-lesion. The protective effects of curcumin were associated to its ability to prevent the quinolinic acid-induced decrease of striatal intra-nuclear Nrf2 levels (30 and 120 min post-lesion), and total superoxide dismutase and glutathione peroxidase activities (1 day post-lesion). Therefore, results of this study support the concept that neuroprotection induced by curcumin is associated with its ability to activate the Nrf2 cytoprotective pathway and to increase the total superoxide dismutase and glutathione peroxidase activities.

© 2013 Elsevier Inc. All rights reserved.

**Keywords:** Nrf2; Curcumin; Quinolinic acid; Oxidative stress

### 1. Introduction

Neurodegeneration is the result of pathological processes producing severe and specific patterns of brain cell damage in a concerted manner [1,2]. Neurodegenerative events constitute a major cause for development of neurological disorders. Human diseases coursing with neurodegeneration involve excitotoxicity as a triggering event for the initiation of deadly cascades [3–5]. Excitotoxicity is currently defined as a toxic process characterized by a sustained stimulation of excitatory amino acid receptors [6–8], mainly involving N-methyl-D-aspartate receptors (NMDAr). Different toxic events derived from excitotoxicity have been characterized in experimental models, and they include upregulation of detrimental signaling pathways, disrupted  $\text{Ca}^{2+}$  homeostasis, and recruitment of reactive oxygen and

nitrogen species (ROS/RNS), with further oxidative/nitrosative stress [2,8–11], ultimately leading to cell death.

Quinolinic acid (QUIN) is a glutamatergic agonist acting on NMDAr, preferentially in discrete populations of these receptors containing the NR2A and NR2B subunits. This metabolite is synthesized in the kynurenine pathway, and is normally present at nanomolar concentrations in human and rat brains [12]. However, under pathological conditions, kynurenine pathway is stimulated to increase the levels of QUIN, therefore augmenting the risk for excitotoxic events. Then, this toxic metabolite exerts excessive excitation of NMDAr and recruits enhanced cytoplasmic  $\text{Ca}^{2+}$  concentrations, mitochondrial dysfunction, decreased ATP levels, cytochrome c release and oxidative stress, further leading to selective loss of GABAergic and cholinergic neurons [13]. Indeed, when injected into the brain, QUIN reproduces neurodegenerative events in rodents, resembling those observed in the brains of patients with Huntington's disease [14]. In addition, the intrastriatal infusion of QUIN to rodents stimulates lipid peroxidation in this region at short times [15], and these findings are related to increased extracellular levels of hydroxyl radical ( $\text{OH}^{\cdot}$ ) in the same brain region [16]. Furthermore, QUIN is known to generate a dysregulation in the oxidant/antioxidant ratio by affecting the

<sup>☆</sup> This work was supported by CONACYT (Grant No. 103527 to PDM and 129838 to JPCH) and by PAPIT IN121910.

\* Corresponding author. Patología Vascular Cerebral, Instituto Nacional de Neurología y Neurocirugía Manuel Velasco Suárez, Insurgentes Sur 3877, México D.F., 14269, México. Tel.: +52 55 5606 3822x2009; fax: +52 55 5424 0808.

E-mail address: [maldonado.perla@gmail.com](mailto:maldonado.perla@gmail.com) (P.D. Maldonado).

reduced glutathione:oxidized glutathione (GSH:GSSG) ratio, as well as depleting the activity of Cu,Zn-SOD at different post-lesion times [17], also recruiting the early and time-dependent formation of peroxynitrite (ONOO<sup>·</sup>) as a key RNS contributing to this paradigm [18]. Noteworthy, these and other alterations induced by QUIN can be prevented by different antioxidants such as melatonin, sodium selenite, L-carnitine, epigallocatechin gallate, etc. [15,19–21]. This evidence highlights a substantial contribution of oxidative stress to the toxic pattern elicited by QUIN. Consequently, it can be assumed that agents exhibiting antioxidant properties may have potential therapeutic value at experimental level in this and other models.

Curcumin (CUR), the polyphenolic non-flavonoid yellow bioactive component of turmeric – the powdered rhizome of *Curcuma longa* Linn –, has been shown to produce a wide range of positive biological effects through its antioxidant and anti-inflammatory properties [22,23]. CUR is non-toxic and has been shown to be a potent free radical scavenger [24,25]. In addition, CUR, like other polyphenols commonly found in plants, fruits and vegetables, competes in efficacy with vitamins C and E [26], although recent findings have attributed part of its anti-inflammatory efficacy to its more stable metabolite tetrahydrocurcumin [27]. Nevertheless, CUR itself has been shown to cross the blood-brain barrier to exert neuroprotective effects, such as those reported against homocysteine-induced cognitive impairment and oxidative stress in rats [25]. CUR also inhibits amyloid toxicity in vivo [28] and improves memory functions in a streptozotocin-induced dementia model in rats through insulin receptors [29]. One of the most relevant findings on CUR research is the description of its capacity to upregulate the master antioxidant coordinator, transcription factor nuclear factor erythroid 2-related factor 2 (Nrf2), which in turn is responsible for phase 2 antioxidant and detoxification genes expression, such as heme oxygenase-1, and this effect of CUR is able to protect the rat brain from focal ischemia [23].

Despite a few groups have already described protective effects of CUR on QUIN-induced toxicity – including antiperoxidative actions in rat brain homogenates [30], as well as antiexcitotoxic and antioxidant effects in primary cultures of human neurons [21] –, to our knowledge there are no reports on the effects of this polyphenolic compound in the toxic model induced by QUIN under in vivo conditions, nor on a possible involvement of Nrf2 in CUR-induced neuroprotection. Therefore, the aim of this work was to evaluate if CUR can attenuate or prevent the QUIN-induced in vivo toxicity in rats, and whether this effect is dependent on Nrf2 upregulation. Our results support a role of the Nrf2 pathway in the neuroprotective actions of CUR in this paradigm.

## 2. Methods and materials

### 2.1. Reagents and chemicals

CUR, QUIN, apomorphine, 2,4-dinitrophenylhydrazine (DNPH), guanidine hydrochloride, 4-(2-hydroxyethyl)-1-piperazineethanesulfonic acid (HEPES), sodium fluoride (NaF), phenylmethylsulfonyl fluoride, sodium pyrophosphate, sodium vanadate (Na<sub>3</sub>VO<sub>4</sub>), ethylenediaminetetraacetic acid (EDTA), ethylene glycol tetraacetic acid (EGTA), Nonidet P-40, glycerol, sodium dodecyl sulfate (SDS), leupeptin, glutathione (GSH), glutathione reductase, NADPH, xanthine, xanthine oxidase, nitroblue tetrazolium (NBT), and bovine serum albumin (BSA), were obtained from Sigma-Aldrich (St. Louis, MO, USA). Fluoro-jade B (F-JB) was obtained from Millipore (Bedford, MA, USA). Anti-Nrf2 antibody used for immunofluorescence (C-20, sc-722) and Western blot (sc-13032), anti-Lamin B1 antibody (sc-20682), and 4',6-diamidino-2-phenylindole dihydrochloride (DAPI, sc-3598) were obtained from Santa Cruz Biotechnology (Santa Cruz, CA, USA). Anti-β-tubulin antibody (ab-11307) was from Abcam (San Francisco, CA, USA). Alexa Fluor 488 goat anti-rabbit IgG secondary antibody was obtained from Invitrogen (Carlsbad, CA, USA). Goat-anti rabbit IgG horseradish peroxidase-conjugate (62-6120) and goat-anti mouse IgG horseradish peroxidase-conjugate (sc-2005) secondary antibodies used for Western blot were from Zymed (San Francisco, CA, USA) and Santa Cruz Biotechnology (Santa Cruz, CA, USA), respectively. Vectashield mounting medium was obtained from Vector Labs (Burlin-

game, CA, USA). All other reagents were purchased from other known commercial sources. Deionized water from a Milli-Q System of Millipore (Bedford, MA, USA) was used for the preparation of all solutions.

### 2.2. Animals

Male Wistar rats initially weighing 250–300 g, were used throughout the study. For all experimental purposes, animals were housed five per cage in acrylic boxes and provided with standard commercial rat chow (Lab Rodent Diet 5001; PMI Feeds Inc., Richmond, IN, USA) and water ad libitum. The housing room was maintained under constant conditions of humidity (50%±10%), temperature (25°C±3°C) and lighting (12 h dark-light cycles). All procedures with animals were carried out strictly according to the National Institutes of Health *Guidelines for the care and use of laboratory animals* and the local guidelines on the ethical use of animals from the Health Ministry of Mexico. During the experiments, all efforts were made to minimize animal suffering.

### 2.3. Experimental design

All experiments were performed during the morning (starting every day at 8:00 AM). The animals were randomly divided into four groups, as mentioned below: 1) control group (CT), treated with vehicle plus saline; 2) CUR group, treated with CUR plus saline; 3) QUIN group, treated with vehicle plus QUIN; and 4) CUR+QUIN group, treated with CUR plus QUIN. Animals from CUR and CUR+QUIN groups received CUR (100, 200 or 400 mg/kg/day, p.o.) for 10 consecutive days. CT and QUIN groups received vehicle for 10 days. CUR was dissolved in carboxymethylcellulose 5% (vehicle). On day 10, animals were intrastriatally infused with 1 μl of QUIN or saline. QUIN-treated rats received a single infusion of QUIN (240 nmol/μl) in the right striatum, according to the following stereotaxic coordinates: +0.5 mm anterior to bregma, -2.6 lateral to bregma, and +4.5 mm ventral to the dura [31]. The effects of increased doses of CUR (100, 200 and 400 mg/kg) on circling behavior (6 days post-lesion) and histological alterations (7 days post-lesion) induced by QUIN were first evaluated to select an optimum protective dose of CUR. The most prominent protective effect was observed with 400 mg/kg, so this dose was used from this point on for further assays. Neurodegeneration (1 and 3 days post-lesion), protein carbonyl levels (6 h post-lesion), Nrf2 activation (30 and 120 min post-lesion), and activities of total superoxide dismutase (SOD) and glutathione peroxidase (GPx) (1 day post-lesion) were determined.

### 2.4. Circling behavior

Motor alterations, assessed as rotation behavior, were evaluated in animals from all experimental groups, according to previous reports [20,32]. Six days after QUIN infusion, animals were administered with apomorphine (1 mg/kg, s.c.) and separated into individual acrylic box cages. Five minutes later, the number of ipsilateral rotations to the lesioned side was recorded for 1 h. Each rotation was defined as a complete turn (360°). Data are expressed as the total number of ipsilateral turns in 1 h.

### 2.5. Histological examination

Brain tissues were collected and histologically processed according to previous descriptions [20,32]. Seven days after intrastriatally lesioned, animals from all groups were anesthetized i.p. with 0.5 mL of sodium pentobarbital and perfused transcardially with 0.9% saline solution containing heparin (200/1 v/v), followed by 4% p-formaldehyde at 4°C. Brains were removed, post-fixed in 4% p-formaldehyde for 7 days and embedded in paraffin. Fixed tissues were serially sectioned in an 820 Histostat microtome (American Instrument Exchange, Inc., Haverhill, MA, USA). Striatal sections (5 μm-thick) were obtained every 100 μm, covering a total distance of 300 μm (100 μm anterior and 100 μm posterior to the needle tract). All sections were stained with hematoxylin-eosin (H&E) to visualize cell bodies, using an image analyzer IM100 (Leica Cambridge, UK).

### 2.6. Quantitative assessment of lesions

Cell counting in histologically prepared sections was performed as previously described [32]. The general criteria to score damaged cells included pyknotic nuclei, cytoplasmic vacuolation, neuronal atrophy, interstitial edema and necrosis. The number of damaged and preserved neurons was obtained from 5 randomly selected fields in three section slides per brain. Data are expressed as percentage of damaged neurons per field.

### 2.7. Detection of neurodegeneration using F-JB staining

Brain tissue was collected and processed according to previous reports [33,34]. One and three days after intrastriatally lesioned, animals from all groups were anesthetized i.p. with 0.5 mL of sodium pentobarbital and transcardially perfused with 0.9% saline solution containing heparin (200/1 v/v), followed by 4% p-formaldehyde at 4°C. Brains were removed and post-fixed in 2% p-formaldehyde and 30% sucrose for 7 days at 4°C. Tissues were then submerged in optimal cutting temperature compound and frozen over liquid nitrogen, followed by cryosection at

-25°C in a cryostat microm HM520 (Thermo Scientific, Pittsburg, PA, USA). Sections (22  $\mu$ m-thick) were mounted onto glass slides coated with 0.5% gelatin and immersed in 1% NaOH and 80% ethanol for 5 min, followed for 2 min in 70% ethanol. Slides were transferred to 0.06% KMnO<sub>4</sub> for 10 min on a shaking table to assess consistent background suppression between sections, and then rinsed in distilled water for 2 min. Sections were stained in a 0.0004% F-JB plus 0.0002% DAPI solution for 20 min. Slides were rinsed thrice with distilled water for 1 min each step. Excess water was removed, placing the sections on a slide warmer at 50°C until fully dry (5–10 min), and then cleared by further immersion in xylene for at least 1 min before cover slipping with a non-aqueous, nonfluorescent plastic mounting media. Immunofluorescence was visualized with an image analyzer IM100 (Leica Cambridge, UK) using a green filter for F-JB and blue filter for DAPI.

#### 2.8. Protein carbonyl content

As an index of protein oxidation, protein carbonyl content in the striatal tissue (6 h post-lesion) was determined as previously described [32]. Assessment of carbonyl formation was done on the basis of formation of protein hydrazone by reaction with DNPH. Striatal homogenates were incubated with 10% streptomycin sulfate to remove nucleic acids overnight and centrifuged at 21,000  $\times$  g at 4°C for 20 min. Further, striatal homogenates were treated with 10 mM DNPH (in 2.5 M HCl) for 1 h at room temperature, and 10% trichloroacetic acid was added and centrifuged at 2,500  $\times$  g at 4°C for 10 min. Pellet was washed three times with ethanol/ethyl acetate (1:1), dissolved with 6 M guanidine hydrochloride (in phosphate buffer 20 mM, pH 7.4), and centrifuged at 5,000  $\times$  g at 4°C for 3 min to remove insoluble material. Absorbance was measured at 370 nm. Protein carbonyl content is expressed as nmol DNPH/mg protein, using the molar absorption coefficient of DNPH (22,000 M<sup>-1</sup> cm<sup>-1</sup>). Total protein concentration was obtained by reading optical density at 280 nm in blank tubes prepared in parallel (treated only with 2.5 M HCl), using a standard curve of BSA (0.25–2 mg/ml) prepared in 6 M guanidine hydrochloride.

#### 2.9. Detection of Nrf2 by immunofluorescence

Thirty and 120 min after intrastriatally lesioned, animals from all groups were anesthetized with 0.5 mL sodium pentobarbital and transcardially perfused with 0.9% saline solution containing heparin (200/1 v/v), followed by 4% p-formaldehyde at 4°C. Brains were removed, post-fixed in a solution of 2% p-formaldehyde and 30% sucrose for 10 days. Then, tissues were submerged in optimal cutting temperature compound and frozen over liquid nitrogen, followed by cryosection at -25°C in a cryostat microm HM520 (Thermo Scientific, USA). Sections (6–10  $\mu$ m-thick) were mounted onto glass slides coated with 0.5% gelatin, permeabilized with 0.1% triton for 10 min and incubated with 5% BSA in PBS to block non-specific immunoreactivity for 1.5 h at room temperature. Slides were incubated with anti-Nrf2 antibody in 5% BSA (1:100) overnight at 4°C, and then incubated with Alexa Fluor 488 goat anti-rabbit secondary antibody in 5% BSA (1:500) for 1 h at room temperature. Finally, the slides were incubated with DAPI (1:1,000) for 10 min to stain nuclei and mounted in medium Vectashield. Immunofluorescence was visualized using an image analyzer IM100 (Leica Cambridge, UK) using a green filter for detection of Nrf2 positive cells and blue filter for DAPI. Data are expressed as positive cells to Nrf2 and the intra-, peri- or extra-nuclear localizations are indicated.

#### 2.10. Preparation of cytosolic/nuclear fractions and quantification of Nrf2 by Western blot

Striatal tissue was washed once with cold PBS and lysed on ice with cold buffer A (250 mM sucrose, 20 mM HEPES pH = 7.0, 0.15 mM EDTA, 0.015 mM EGTA, 10 mM

KCl, 1 mM phenylmethylsulfonyl fluoride, 20 mM NaF, 1 mM sodium pyrophosphate, 1 mM Na<sub>3</sub>VO<sub>4</sub>, 1% Nonidet P-40, and 1  $\mu$ g/mL leupeptin). Homogenates were then centrifuged at 500  $\times$  g for 5 min, the supernatants were recovered as cytosolic fractions, and the nuclear pellets were washed in cold buffer B (10 mM HEPES pH = 8.0, 0.1 mM EDTA, 1 mM phenylmethylsulfonyl fluoride, 20 mM NaF, 1 mM sodium pyrophosphate, 1 mM Na<sub>3</sub>VO<sub>4</sub>, 25% glycerol, 0.1 M NaCl, and 1  $\mu$ g/mL leupeptin). After a second step of centrifugation at 500  $\times$  g for 5 min, the nuclei were resuspended in 2% SDS hypertonc cold buffer C (10 mM HEPES pH = 8.0, 0.1 mM EDTA, 1 mM phenylmethylsulfonyl fluoride, 20 mM NaF, 1 mM sodium pyrophosphate, 1 mM Na<sub>3</sub>VO<sub>4</sub>, 25% glycerol, 0.4 M NaCl, and 1  $\mu$ g/mL leupeptin), and sonicated. Cytosolic and nuclear fractions were resolved in SDS-PAGE (10%), using 60  $\mu$ g (cytoplasmic fraction) or 80  $\mu$ g (nuclear fraction) protein/lane, transferred into Immobilon-P membranes (PVDF, Millipore), and immunoblotted with primary antibodies: anti-Nrf2, anti- $\beta$ -tubulin and anti-Lamin B1 (1:1,000). Peroxidase-conjugated secondary antibodies (1:10,000) were used to detect the proteins of interest by enhanced chemiluminescence, according to a previous report [35]. The corresponding bands were quantified by densitometry.

#### 2.11. SOD activity

Total SOD activity (MnSOD and CuZnSOD) in homogenates was determined using xanthine-xanthine oxidase system to reduce NBT. Mixture reaction contained in a final concentration: 0.122 mM EDTA, 30.6  $\mu$ M NBT, 0.122 mM xanthine, 0.006% BSA, and 49 mM sodium carbonate. Five hundred  $\mu$ l of homogenates (1:20) were added to 2.45 ml of the mixture described above, then 50  $\mu$ l xanthine oxidase, in a final concentration of 2.8 U/l, were added and incubated in a water bath at 27°C for 30 min. The reaction was stopped with 1 ml of 0.8 mM cupric chloride and the optical density was read at 560 nm. One hundred percent of NBT reduction was obtained in a tube in which the sample was replaced by distilled water. The amount of protein that inhibited NBT reduction to 50% of maximum was defined as one unit of SOD activity. Results were expressed as U/mg protein.

#### 2.12. GPx activity

Reaction mixture consisted of 50 mM potassium phosphate pH = 7.0, 1 mM EDTA, 1 mM NaN<sub>3</sub>, 0.2 mM NADPH, 1 U/ml of glutathione reductase, and 1 mM GSH. One hundred  $\mu$ l of homogenates were added to 0.8 ml of mixture and allowed to incubate for 5 min at room temperature before initiation of the reaction by the addition of 0.1 ml 0.25 mM H<sub>2</sub>O<sub>2</sub> solution. Absorbance at 340 nm was recorded for 5 min, and the activity was calculated from the slope of these lines as  $\mu$ moles of NADPH oxidized per min. Blank reactions with homogenates replaced by distilled water were subtracted from each assay. GPx activity was expressed as U/mg protein.

#### 2.13. Statistical analysis

All results are presented as mean values  $\pm$  SEM. Data were analyzed by one-way ANOVA followed by post-hoc Tukey's test, using the software Prism 5.0 (GraphPad, San Diego, CA, USA). Values of  $P$  < .05 were considered statistically significant.

### 3. Results

#### 3.1. CUR treatment diminished the rotational behavior induced by QUIN

QUIN group reached an average of 233  $\pm$  66 ipsilateral turns, whereas CUR treatment significantly attenuated this marker since a dose of 100 mg/kg (CUR100+QUIN: 155  $\pm$  25 ipsilateral turns). The most prominent protective effect was observed with 400 mg/kg (CUR400 + QUIN: 54  $\pm$  14 ipsilateral turns). Neither CT, nor CUR400 groups exhibited any circling behavior after apomorphine challenge (Fig. 1).

#### 3.2. CUR treatment prevented the histological damage and neurodegeneration induced by QUIN in the striatum

In contrast to the well-preserved appearance of the striatal tissues from CT animals, the infusion of QUIN resulted in cellular damage revealed by extensive neuronal cell loss along the dorsal striatum, abundant pyknosis, shrunken cells, retraction of neuropil and interstitial edema. All CUR doses tested were able to prevent the morphological alterations evoked by QUIN (Fig. 2, upper panel). The administration of CUR alone presented a normal appearance of striatal tissue similar to that of CT group. These findings were strengthened by the quantitative assessment of nerve tissue damage.

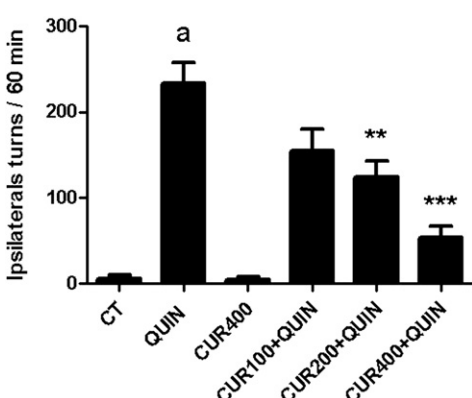


Fig. 1. Effect of curcumin (CUR) on quinolinic acid (QUIN)-induced rotation behavior. CT: control group. Doses of CUR were 100, 200 and 400 mg/kg. Data are expressed as mean values  $\pm$  SEM. n = 6. <sup>a</sup>P < .001 vs. CT, <sup>\*\*</sup>P < .01 and <sup>\*\*\*</sup>P < .001 vs. QUIN.

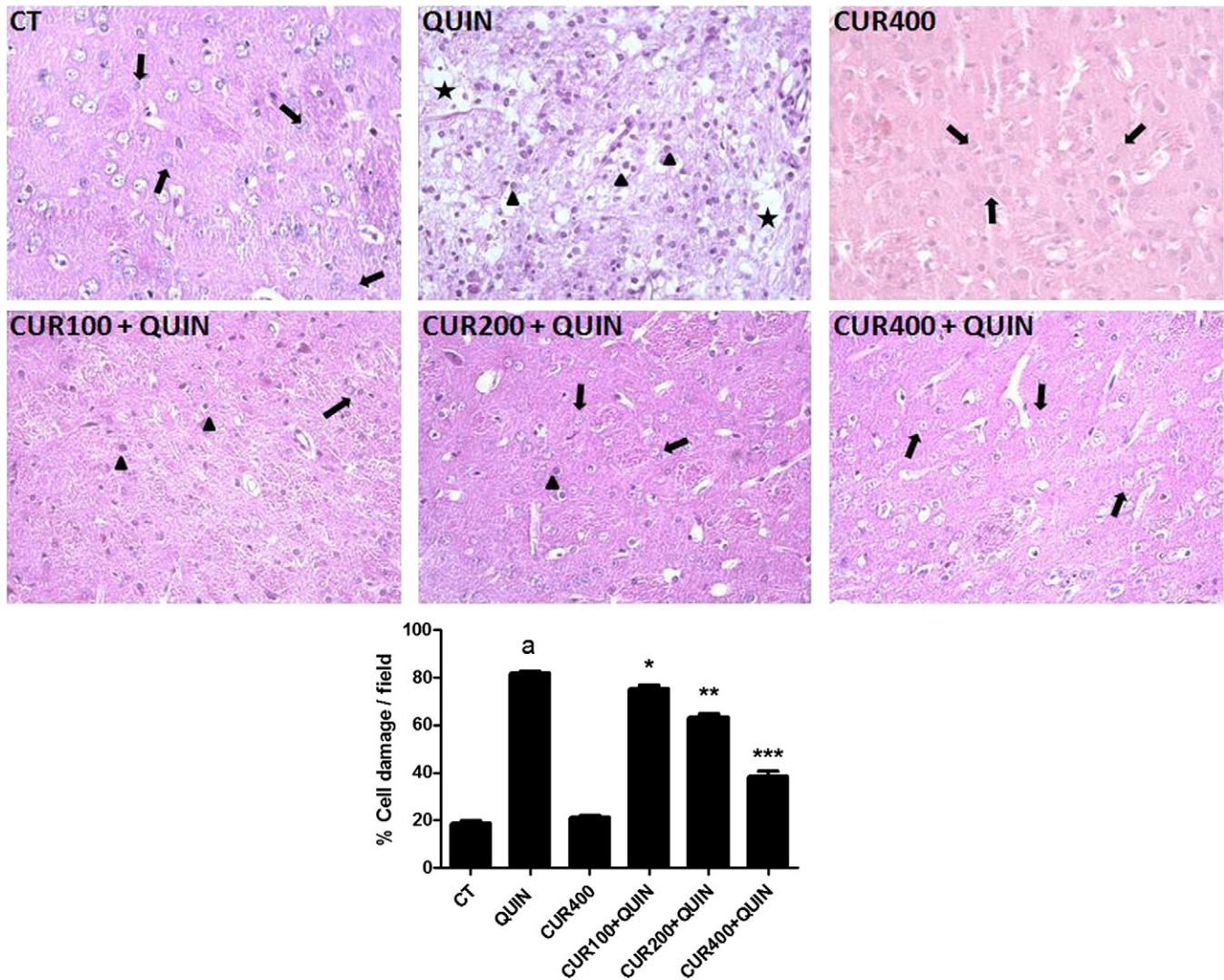


Fig. 2. Effect of curcumin (CUR) on quinolitic acid (QUIN)-induced neuronal damage in the rat striatum. Five- $\mu$ m thick sections were stained with hematoxylin-eosin and observed under light microscopy. Representative photomicrographs of each group are shown in upper panel. Interstitial edema and retracted neuropil (black stars), pyknotic nuclei (black triangles), and preserved cells (black arrows) are shown. Graph shows the damaged cell counting. CT: control group. Doses of CUR were 100, 200 and 400 mg/kg. Data are expressed as mean values  $\pm$  SEM.  $n=6$ .  $^a$  $P<.001$  vs CT,  $^*P<.05$ ,  $^{**}P<.01$  and  $^{***}P<.001$  vs. QUIN.

Animals from the CUR100 + QUIN group showed a decrease of 8% in the number of damaged cells per field produced by QUIN in the striatum, but the most prominent neuroprotective effect was observed in the CUR400 + QUIN group, showing a decrease of 53% (Fig. 2, lower panel).

F-JB staining for assessment of neurodegeneration at 1 and 3 days post-lesion is shown in Fig. 3, upper and lower panel, respectively. CT and CUR groups virtually showed no fluorescence in striatal tissue, while rats treated with QUIN exhibited an abundant fluorescence associated with positivity to F-JB, suggesting degeneration of striatal cells. Animals treated with CUR and exposed to QUIN presented less fluorescence than the QUIN group alone, although these tissues still displayed some fluorescence, thus suggesting that degenerative events remained active.

### 3.3. QUIN-induced oxidative stress was decreased by CUR treatment

Administration of QUIN to rats increased the striatal protein carbonyl content by 157% above the CT group, whereas CUR treatment decreased the QUIN-induced protein carbonyl content to

basal levels (Fig. 4). Animals receiving CUR alone exhibited no significant changes.

### 3.4. CUR treatment increased Nrf2 levels and prevented the decrease in Nrf2 induced by QUIN

We examined the immunolocalization of Nrf2 protein at 30 (Fig. 5, upper panel) and 120 min (Fig. 6, upper panel) after QUIN or saline infusion. Quantification of positive cells to Nrf2 showed that QUIN treatment diminished the intra-nuclear localization of Nrf2 by 62% at 30 min, and 76% at 120 min, while increased its peri- and extra-nuclear localization compared to CT group. CUR administration prevented this decrease above basal levels. CUR alone significantly increased intra-nuclear Nrf2 localization by 113% at 30 min, and 69% at 120 min, when compared to control group (Figs. 5 and 6, lower panel). Similar results were observed by Western blot: QUIN administration decreased the cytosolic Nrf2 levels by 43.6% and 51.8% at 30 and 120 min, respectively (Fig. 7A), and depleted nuclear Nrf2 levels by 55.5% and 65.4% at 30 and 120 min, respectively (Fig. 7B). CUR treatment prevented this decrease above basal levels

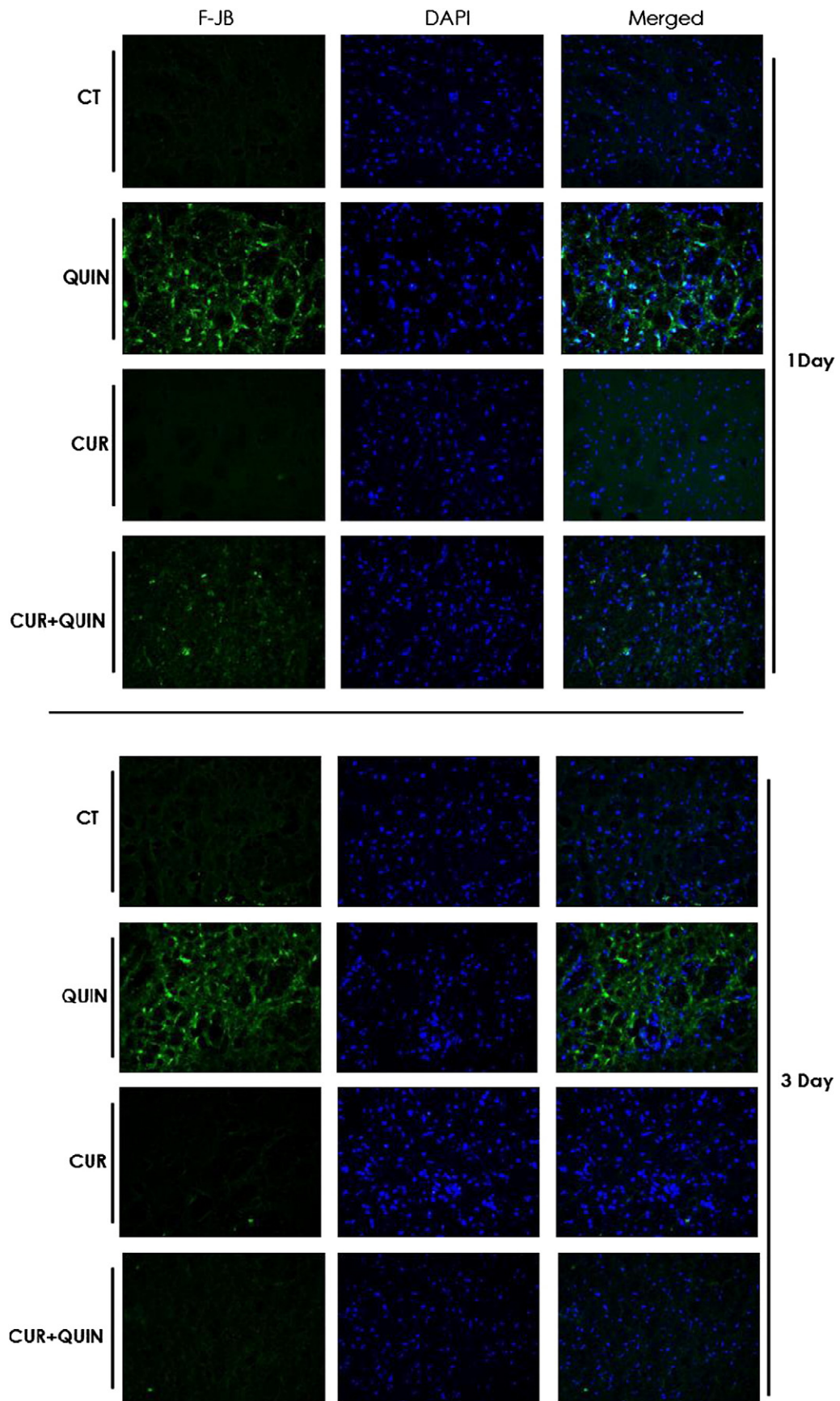


Fig. 3. Effect of curcumin (CUR) on quinolinic acid (QUIN)-induced neurodegeneration at 1 (upper panel) and 3 days (lower panel) post-lesion. Twenty-two- $\mu$ m thick sections were stained with fluorojade-B (FJ-B) and DAPI for evidencing positive nuclei. Green fluorescence is proportional to neuronal degeneration.

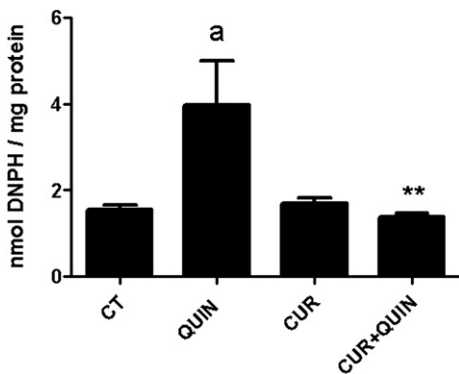


Fig. 4. Effect of curcumin (CUR) on quinolinic acid (QUIN)-induced protein oxidation (measured as protein carbonyl content). CT: control group. Data are expressed as mean values  $\pm$  SEM.  $n = 6$ .  $^aP < .05$  vs. CT,  $^{**}P < .01$  vs. QUIN.

(nuclear Nrf2). In turn, CUR alone increased cytosolic Nrf2 levels by 159.2% and 98.2% at 30 and 120 min, respectively (Fig. 7A), and enhanced nuclear Nrf2 levels by 171% and 163.3% at 130 and 20 min, respectively (Fig. 7B).

### 3.5. CUR treatment increased total SOD and GPx activities and prevented the QUIN-induced decrease in total SOD and GPx activities

QUIN administration decreased the activity of total SOD (28%) and GPx (20%) when compared with the CT group, whereas CUR treatment prevented this decrease down to basal levels. CUR alone increased the activity of total SOD (129%), and to a lesser extent GPx activity (30%) compared to CT group (Table 1).

## 4. Discussion

While redox activity is necessary for the development and adequate functioning of the brain, the central nervous system (CNS) is particularly susceptible to be attacked by ROS/RNS due to a limited antioxidant defense system, a high demand of oxygen accompanied by a considerable dependency on a redox metabolism, and an enriched content of polyunsaturated fatty acid chains in cell membranes [36]. It is therefore accepted that even though the brain possesses endogenous tools to handle and use ROS for its own benefit, when toxic conditions create scenarios of triggered intracellular deleterious signals and aberrant oxidative activity, excessive ROS lead to cell damage and death. The pro-oxidant activity of QUIN is well documented: is known to induce lipid peroxidation [37], increases OH<sup>·</sup> production [16], activates NADPH oxidase [32], nitric oxide synthase [38], and poly(ADP-ribose) polymerase-1 [39], and increases the intracellular Ca<sup>2+</sup> concentration [40], hence generating a highly oxidizing profile. Oxidative and nitrosative stress can cause deleterious effects in cells, especially for its ability to damage biomolecules such as DNA, lipids and proteins. When the later are damaged, either by direct effect of ROS or by products of lipid peroxidation [41], the amount of carbonyl groups in side chains, especially in histidine and cysteine residues, is increased, further leading to its inactivation [42]. It is known that QUIN infusion increases the protein carbonyl content since 3 h post-lesion [32], and here we observed that this marker remained high at 6 h (Fig. 4). This suggests that lesioned tissue is constantly subjected to oxidative stress in this toxic model. In this regard, CUR treatment prevented the increase in oxidized proteins, therefore suggesting that this antioxidant is able to reduce a wide spectrum of oxidative events that are generated after QUIN intrastriatal infusion. A few groups have already

described protective effects of CUR on QUIN-induced toxicity in vitro, and this protection has been associated to its direct antioxidant properties. For instance, Dairam et al. [30] showed the in vitro antioxidant and metal-binding properties of CUR, and postulated it as an important tool for the prevention or attenuation of neurodegenerative diseases, such as Alzheimer disease. Shortly thereafter, Braidy et al. [21] reported the antiexcitotoxic and antioxidant effects of CUR in primary cultures of human neurons treated with QUIN. However, to our knowledge this is the first report on the effect of this polyphenolic compound (CUR) in the toxic model induced by QUIN under in vivo conditions.

In previous studies, it has been shown that the unilateral intrastriatal infusion of glutamate agonists to nerve tissue of animals induces deafferentation of the dopaminergic system and striatal degeneration, causing hypersensitivity to dopamine receptors [7,43]. The subsequent systemic administration of dopamine agonists causes hyperactivation of dopamine receptors in the injured hemisphere, thereby inducing circling behavior due to neurochemical imbalance. In the experimental model produced by QUIN, it has been shown that the subcutaneous administration of apomorphine induces an increase in the number of ipsilateral turns at 6 days after the intrastriatal lesion [37,44]. In turn, CUR administration prevented the increase in the number of ipsilateral turns in a dose-dependent manner (Fig. 1). These results are consistent with other models of excitotoxicity [25] demonstrating that CUR (50 mg/kg) ameliorates neurotoxicity and improves learning and memory deficits by protecting the nervous system against homocysteine toxicity. In this regard, it has been shown that pretreatment with an antioxidant can prevent the behavioral alterations induced in the model with QUIN [15].

During the occurrence of excitotoxic events, overactivation of NMDAr causes ion entry into the cell, including Na<sup>+</sup> and Ca<sup>2+</sup>, thereby causing an osmotic imbalance that eventually induces rupture and cell death [45]. QUIN is a glutamatergic agonist acting on the NR2B subunit of NMDAr and its intrastriatal infusion leads to overactivation of these receptors, allowing the massive entry of Ca<sup>2+</sup> and unleashing a series of events that eventually culminate in cell death [18,46]. This process is intimately linked to neurodegenerative disorders and causes loss of function and neuronal death by necrosis or apoptosis [47]. In this study, pretreatment with CUR to rats improved cell viability and prevented the histological changes characteristic of QUIN-induced neurotoxicity in a dose-dependent manner (Fig. 2). Considering that CUR exerted a neuroprotective effect – mainly at high doses –, we decided to use a 400 mg/kg dose for subsequent experiments. CUR treatment significantly prevented the QUIN-induced neurodegeneration, especially at 3 days after the intrastriatal infusion of QUIN. Noteworthy, QUIN promoted rapid neurodegeneration in a manner that was sustained over time (Fig. 3), thus implying that those QUIN toxic effects responsible for neurodegeneration are occurring at early times after its infusion.

Despite the protective effect of CUR on QUIN-induced neurotoxicity has previously been associated with its direct antioxidant properties – an effect that should be not discarded at all [30] –, in this study we explored the possible involvement of Nrf2 signaling pathway in CUR-induced neuroprotection. Subcellular localization of Nrf2 shows that, under physiological conditions, Nrf2 is present both inside and outside the nucleus, thus suggesting a balanced dynamics of active/inactive forms; however, during excitotoxic conditions, Nrf2 levels are significantly reduced in the nucleus (Fig. 5, 6 and 7). These findings suggest that QUIN induces Nrf2 degradation and avoids its internalization to the nucleus. This is relevant since it would be expected that, in response to oxidative stress induced by QUIN, Nrf2 could be translocated from the cytoplasm into the nucleus and transactivates the expression of genes with antioxidant activity, but this is not really occurring, or not at least under the

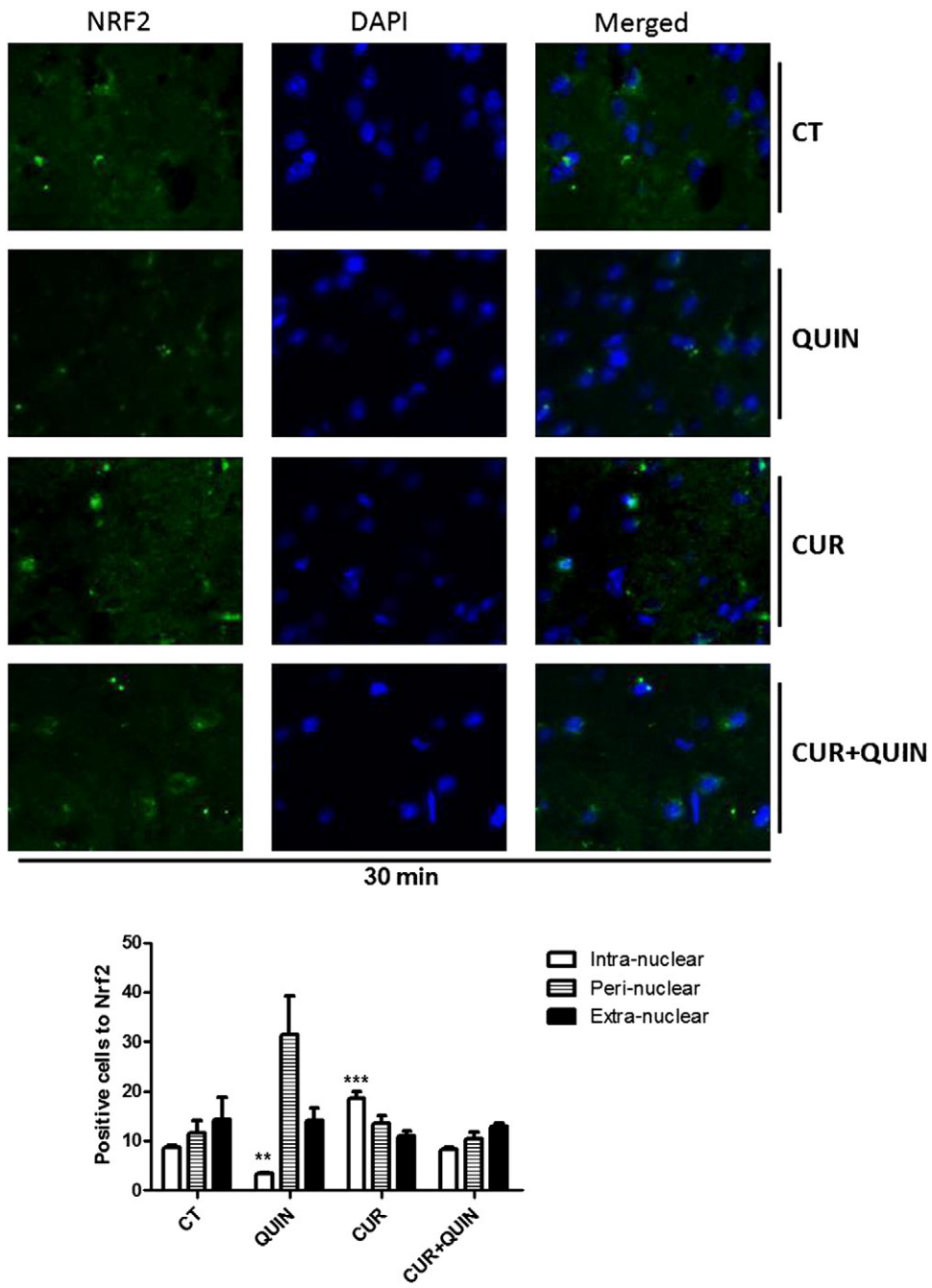


Fig. 5. Effect of curcumin (CUR) on induction of transcription factor Nrf2 at 30 min after the intrastratal infusion of quinolinic acid (QUIN) to rats. Upper panel shows representative photomicrographs for each group; positive cells to Nrf2 are shown in green and stained nuclei are shown in blue. The right column is a merge of Nrf2 with DAPI. Graph shows counting of positive cells to Nrf2 and localization with respect to nuclei. Data are expressed as mean values  $\pm$  SEM.  $n = 3$ . \*\* $P < .01$  and \*\*\* $P < .001$  vs CT group.

toxic conditions employed in this study. Instead, our findings are in agreement with those reported by Ramsey et al. [48], who found that Nrf2-mediated transcription is not induced in neurons of Alzheimer's disease *postmortem* tissues. In contrast, in Parkinson's disease, nuclear localization of Nrf2 is strongly induced, but this response is apparently insufficient to protect neurons from oxidative degeneration. We therefore hypothesize that the toxic insult induced by 240 nmol QUIN is strong enough to silence Nrf2 translocation, therefore avoiding any compensatory response to the toxic condition. Moreover, our data suggests that Nrf2 transactivation induced by compounds such as CUR could be a potential therapeutic target as it was capable of inducing Nrf2 signaling

pathway to exert neuroprotection. This appreciation is based on the fact that CUR treatment prevented the reduction of the active form of Nrf2 (intra-nuclear localization) observed in QUIN treated rats, and this effect could be associated with the ability of CUR to promote an increase in the active form of Nrf2 (Fig. 5, 6 and 7), the one responsible for the generation of an antioxidant environment for cells. These results are consistent with those reported by Yang et al. [23], who showed that CUR is able to induce the active form of Nrf2 in a model of cerebral ischemia, especially at high doses (100 mg/kg).

In addition, the fact that CUR can act as an indirect antioxidant through its ability to induce Nrf2 transactivation is particularly

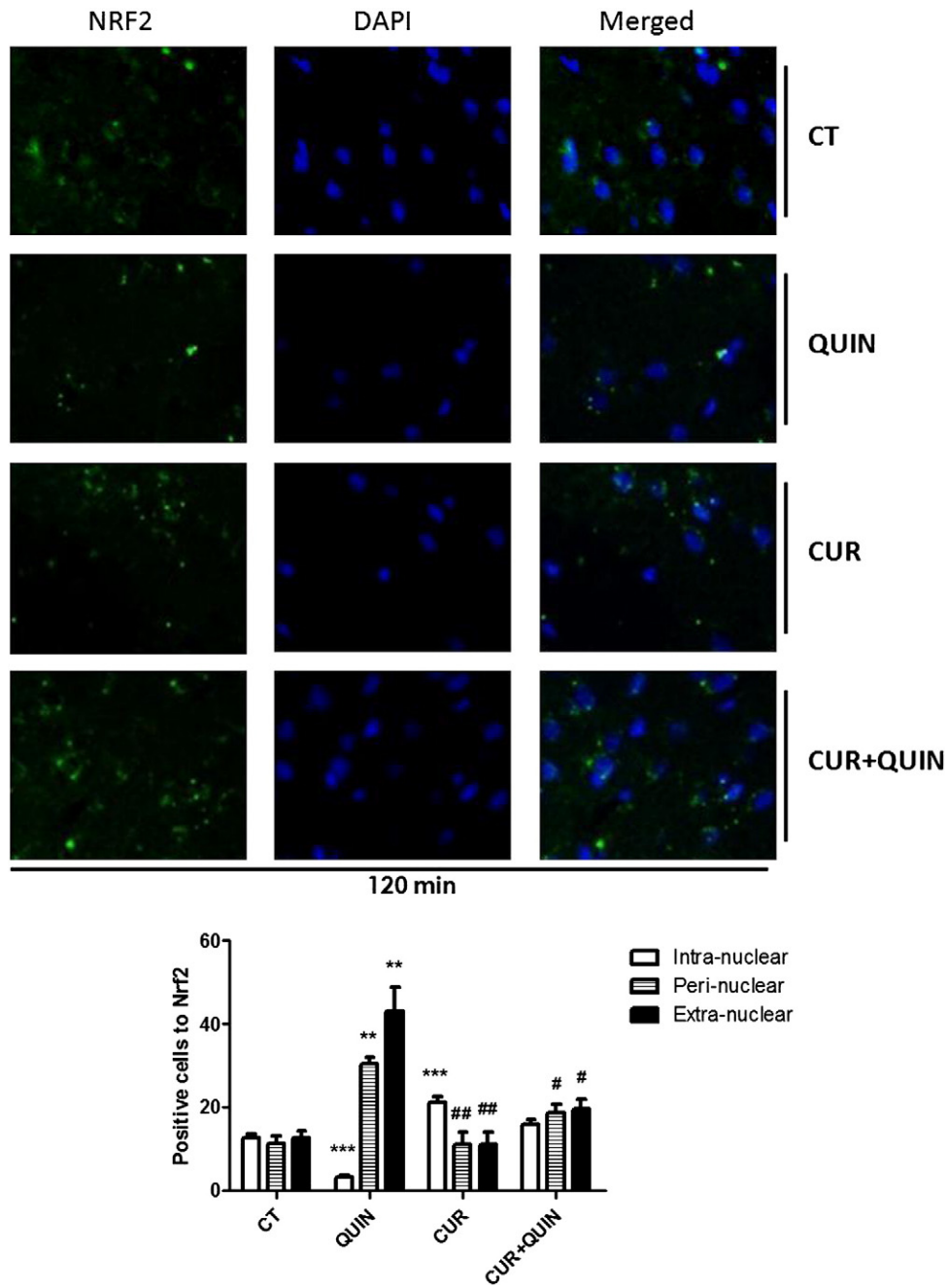


Fig. 6. Effect of curcumin (CUR) on induction of transcription factor Nrf2 at 120 min after the intrastriatal infusion of quinolinic acid (QUIN) to rats. Upper panel shows representative photomicrographs for each group; positive cells to Nrf2 are shown in green and stained nuclei are shown in blue. The right column is a merge of Nrf2 with DAPI. Graph shows counting of positive cells to Nrf2 and localization with respect to nuclei. Data are expressed as mean values  $\pm$  SEM. n = 3. \*\*P<.01 and \*\*\*P<.001 vs. CT, #P<.05 and ##P<.01 vs. QUIN.

relevant since this evidence adds major protective properties to this molecule, a compound that has been assumed to act typically as free radical scavenger and traditional antioxidant. Nrf2 activation stimulates cytoprotective vitagenes involved in antioxidant defense, and these enzymes act catalytically, are not consumed, have a relatively high average life, and catalyze a wide variety of chemical reactions that invariably lead to the detoxification of oxidants and electrophiles [49]. Relevance is also added to the case of neurodegenerative diseases, in which not all neuroprotective therapies have shown efficacy this far [50]. In particular, the brain is susceptible to oxidative damage and has shown low basal levels of Nrf2 [51,52]. This factor

binds to the antioxidant response element (ARE) to activate transcription of proteins necessary for the maintenance and response of cellular defense systems, such as detoxifying enzymes, glutathione-related proteins, antioxidant and anti-inflammatory elements, and NADPH-producing enzymes [53]. Noteworthy, in this work CUR alone increased the activity of total SOD and GPx, and prevented the QUIN-induced decrease in the activity of these enzymes (Table 1). SOD is known to degrade superoxide anion to hydrogen peroxide, which in turn can be catabolized to water by GPx. Both enzymes are induced by Nrf2 and are likely to be involved in the protective effect induced by CUR in the QUIN model. Similar results have been reported in other

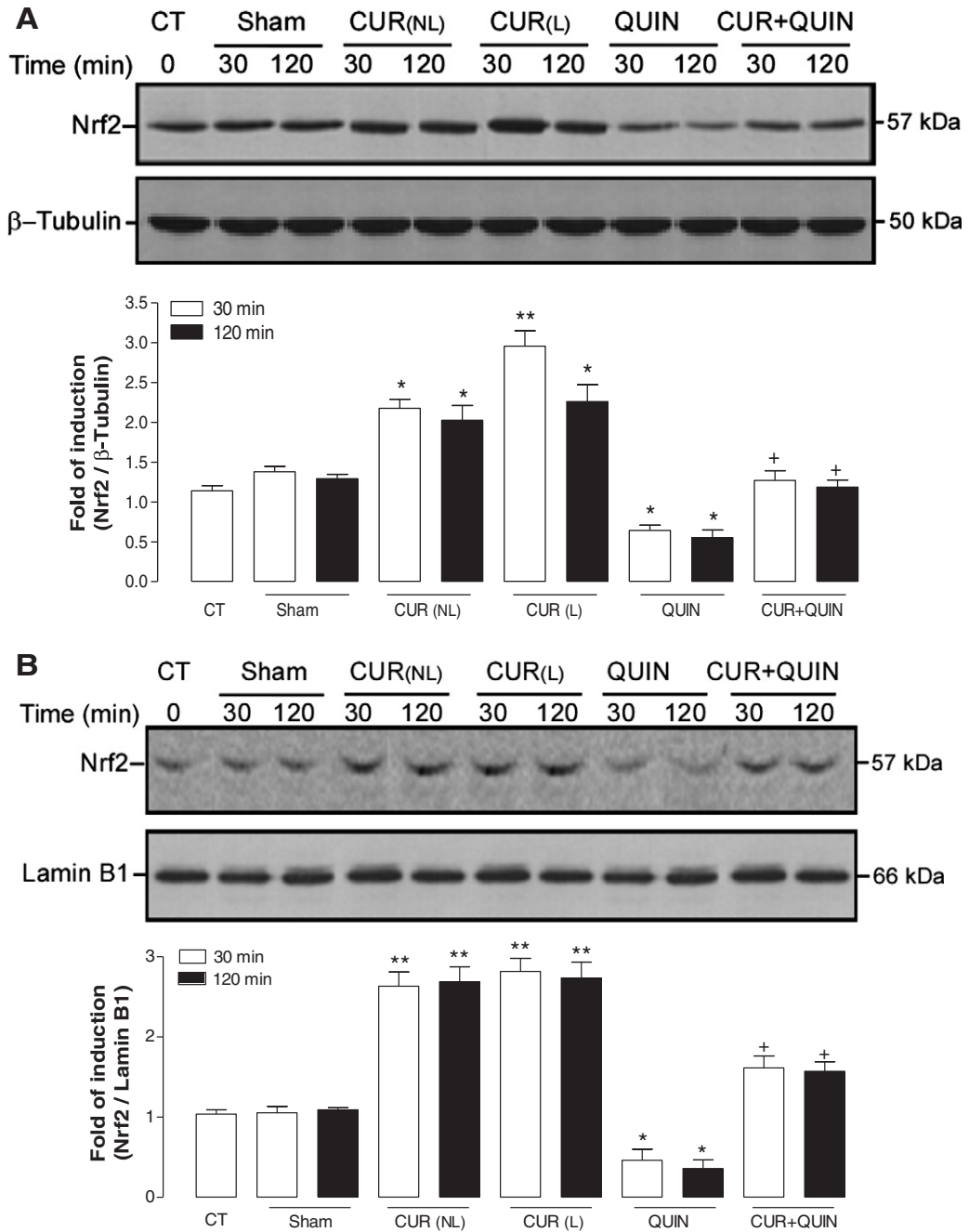


Fig. 7. Effect of curcumin (CUR) on induction of transcription factor Nrf2 at 30 and 120 min after the intrastratial infusion of quinolinic acid (QUIN) to rats by Western blot. In A, a representative blot and quantification (graph) of cytosolic Nrf2 levels for each group. In B, a representative blot and quantification (graph) of nuclear Nrf2 levels for each group. NL: Unlesioned. L: Lesioned. Data are expressed as mean values  $\pm$  SEM. n = 3. \*P < .05 and \*\*P < .01 vs. CT, +P < .05 vs. QUIN.

Table 1  
Effect of curcumin (CUR) on total superoxide dismutase (SOD) and glutathione peroxidase (GPx) activities 1 day after the intrastratial infusion of quinolinic acid (QUIN) to rats.

	Total SOD (U/mg protein)	GPx (U/mg protein)
CT	12.5 $\pm$ 0.4	0.010 $\pm$ 0.0004
QUIN	9.0 $\pm$ 1.1 <sup>a</sup>	0.008 $\pm$ 0.0004 <sup>a</sup>
CUR	28.7 $\pm$ 7.0 <sup>b</sup>	0.013 $\pm$ 0.0005 <sup>a</sup>
CUR+QUIN	13.6 $\pm$ 0.6 <sup>c</sup>	0.010 $\pm$ 0.0005 <sup>c</sup>

<sup>a</sup>P < .01 and <sup>b</sup>P < .001 vs. CT group; <sup>c</sup>P < .05 vs. QUIN group.

models, where CUR activates Nrf2 and related signaling through a Keap1/Nrf2/ARE-dependent pathway, thereby inducing the transcription of antioxidant proteins, such as heme oxygenase-1 [54] and glutathione S-transferase [55].

Finally, CUR has the ability to induce Nrf2, a property that, in turn, is closely related to the presence of hydroxyl groups in ortho-position at the aromatic rings, as well as the  $\beta$ -diketone functionality of the compound [56]. This peculiar chemical characteristic of CUR could be related to its ability to induce Nrf2 activation via its interaction with Keap1. Thus, it is plausible to believe that one mechanistic possibility for our model could imply CUR interaction with Cys residues of Keap1 through hydroxyl groups at aromatic

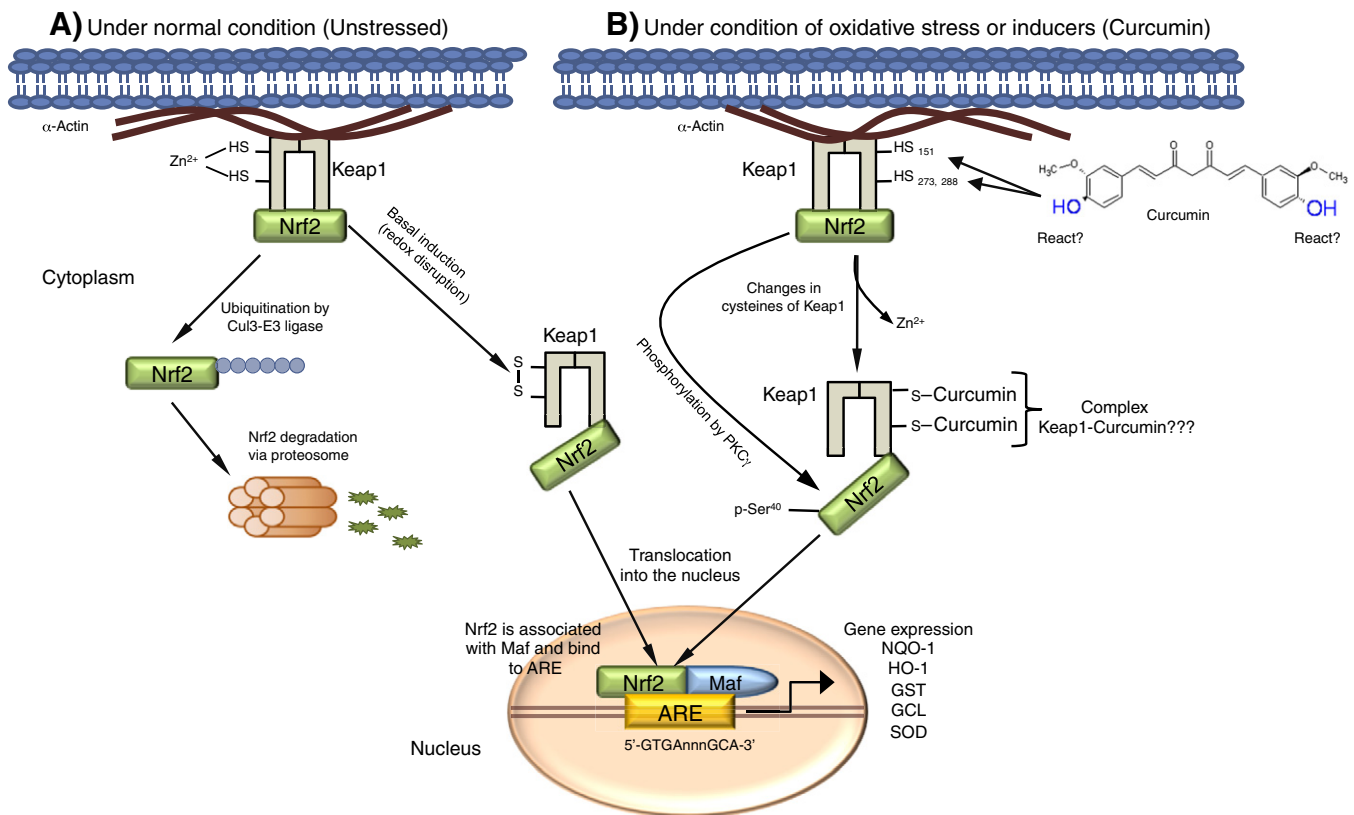


Fig. 8. Possible mechanisms involved in the protective effect of curcumin against neurotoxicity induced by quinolinic acid. A) Under normal condition (unstressed): Keap1 sequesters Nrf2 in the cytoplasm by binding to the actin cytoskeleton. Nrf2 is constantly ubiquitinated by the Culin 3 (Cul3)-Keap1 ubiquitin E3 ligase complex and is degraded in the proteasome. B) Under oxidative stress or inducers (e.g. curcumin): Inducers react covalently with specific cysteine residues in Keap1 (C151, C273 and C288), which abrogates the E3 ligase activity of the Cul3-Keap1 complex. Consequently Nrf2 is stabilized and translocated into the nucleus, where it induces the transcription of various cytoprotective genes (antioxidant enzymes). Nrf2 may also be phosphorylated at Ser40 by PKC $\gamma$ . Nrf2: Nuclear factor (erythroid-derived 2)-like 2; Keap1: Kelch like-ECH-associated protein 1; ARE: Antioxidant response element; PKC $\gamma$ : protein kinase C $\gamma$ ; Maf: muscle aponeurotic fibrosarcoma protein; NQO-1: NAD(P)H dehydrogenase (quinone)-1; HO-1: Heme-oxygenase 1; GST: glutathione-S-transferase; GCL: glutamate cysteine ligase; SOD: superoxide dismutase.

rings to cause a conformational change and further release of Nrf2, which will be translocated into the nucleus (Fig. 8), as has been observed with other inducers of Nrf2, such as sulforaphane [57]. Nevertheless, studies are needed to clarify the precise mechanism of action inherent to CUR through Nrf2/ARE pathway.

## References

- [1] Coyle JT, Puttfarcken P. Oxidative stress, glutamate, and neurodegenerative disorders. *Science* 1993;262:689–95.
- [2] Santamaría A, Jiménez ME. Oxidative/nitrosative stress, a common factor in different neurotoxic paradigms: an overview. *Curr Topics Neurochem Res Trends* 2005;4:1–20.
- [3] Brouillet E, Conde F, Beal MF, Hantraye P. Replicating Huntington's disease phenotype in experimental animals. *Prog Neurobiol* 1999;59:427–68.
- [4] Cowan CM, Raymond LA. Selective neuronal degeneration in Huntington's disease. *Curr Top Dev Biol* 2006;75:25–71.
- [5] Nakamura K, Animoff MJ. Huntington's disease: clinical characteristics, pathogenesis and therapies. *Drugs Today (Barc)* 2007;43:97–116.
- [6] Olney JW, Adamo NJ, Ratner A. Monosodium glutamate effects. *Science* 1971;172:294.
- [7] Schwarcz R, Scholz D, Coyle JT. Structure-activity relations for the neurotoxicity of kainic acid derivatives and glutamate analogues. *Neuropharmacology* 1978;17:145–51.
- [8] Nicholls DG, Johnson-Cadwell L, Vesce S, Jekabsons M, Yadava N. Bioenergetics of mitochondria in cultured neurons and their role in glutamate excitotoxicity. *J Neurosci Res* 2007;85:3206–12.
- [9] Beal MF. Mitochondrial dysfunction and oxidative damage in Alzheimer's and Parkinson's diseases and coenzyme Q10 as a potential treatment. *J Bioenerg Biomembr* 2004;36:381–6.
- [10] Lin MT, Beal MF. Mitochondrial dysfunction and oxidative stress in neurodegenerative diseases. *Nature* 2006;443:787–95.
- [11] Sas K, Robotka H, Toldi J, Vécsei L. Mitochondria, metabolic disturbances, oxidative stress and the kynurenine system, with focus on neurodegenerative disorders. *J Neurol Sci* 2007;257:221–39.
- [12] Chen Y, Guillemin GJ. Kynurene pathway metabolites in humans: Disease and Healthy states. *Int J Tryptophan Res* 2009;2:1–19.
- [13] Pérez-De La Cruz V, Königsberg M, Santamaría A. Kynurene pathway and disease: an overview. *CNS Neurol Disord Drug Targets* 2007;6:398–410.
- [14] McLin JP, Thompson LM, Steward O. Differential susceptibility to striatal neurodegeneration induced by quinolinic acid and kainate in inbred, outbred and hybrid mouse strains. *Eur J Neurosci* 2006;24:3134–40.
- [15] Santamaría A, Salvatierra-Sánchez R, Vázquez-Román B, Santiago-López D, Villeda-Hernández J, Galván-Arzate S, et al. Protective effects of the antioxidant selenium on quinolinic acid-induced neurotoxicity in rats: in vitro and in vivo studies. *J Neurochem* 2003;86:479–88.
- [16] Santamaría A, Jiménez-Capdeville ME, Camacho A, Rodríguez-Martínez E, Flores A, Galván-Arzate S. In vivo hydroxyl radical formation after quinolinic acid infusion into rat corpus striatum. *Neuroreport* 2001;12:2693–6.
- [17] Rodríguez-Martínez E, Camacho A, Maldonado PD, Pedraza-Chaverrí J, Santamaría D, Galván-Arzate S, et al. Effect of quinolinic acid on endogenous antioxidants in rat corpus striatum. *Brain Res* 2000;858:436–9.
- [18] Pérez-De La Cruz V, González-Cortés C, Galván-Arzate S, Medina-Campos ON, Pérez-Severiano F, Ali SF, et al. Excitotoxic brain damage involves early peroxynitrite formation in a model of Huntington's disease in rats: protective role of iron porphyrinate 5,10,15,20-tetrakis (4-sulfonophenyl) porphyrinate iron (III). *Neuroscience* 2005;135:463–74.
- [19] Behan WM, McDonald M, Darlington LG, Stone TW. Oxidative stress as a mechanism for quinolinic acid-induced hippocampal damage: protection by melatonin and deprenyl. *Br J Pharmacol* 1999;128:1754–60.
- [20] Silva-Adaya D, Pérez-De La Cruz V, Herrera-Mundo MN, Mendoza-Macedo K, Villeda-Hernández J, Binienda Z, et al. Excitotoxic damage, disrupted energy metabolism, and oxidative stress in the rat brain: antioxidant and neuroprotective effects of L-carnitine. *J Neurochem* 2008;105:677–89.
- [21] Braidy N, Grant R, Adams S, Guillemin GJ. Neuroprotective effects of naturally occurring polyphenols on quinolinic acid-induced excitotoxicity in human neurons. *FEBS J* 2010;277:368–82.

[22] Al-Omar FA, Nagi MN, Abdulgadir MM, Al-Joni KS, Al-Majed AA. Immediate and delayed treatments with curcumin prevents forebrain ischemia-induced neuronal damage and oxidative insult in the rat hippocampus. *Neurochem Res* 2006;31:611–8.

[23] Yang C, Zhang X, Fan H, Liu Y. Curcumin upregulates transcription factor Nrf2, HO-1 expression and protects rat brains against focal ischemia. *Brain Res* 2009;1282:133–41.

[24] Pan R, Qiu S, DX LU, Dong J. Curcumin improves learning and memory ability and its neuroprotective mechanism in mice. *Chin Med J* 2008;121:832–9.

[25] Ataie A, Sabetkasaie M, Haghparast A, Hajizadeh Moghaddam A, Kazeminejad B. Neuroprotective effects of the polyphenolic antioxidant agent, Curcumin, against homocysteine-induced cognitive impairment and oxidative stress in the rat. *Pharmacol Biochem Behav* 2010;96:378–85.

[26] Blumenthal M, Goldberg A, Brinkman J. *Herbal Medicine: the expanded commission E monographs*. Newton MA: Integrative Medicine Communications; 2000. p. 330–4.

[27] Begum AN, Jones MR, Lim GP, Morihara T, Kim P, Heath DD, et al. Curcumin structure-function, bioavailability, and efficacy in models of neuroinflammation and Alzheimer's disease. *J Pharmacol Exp Ther* 2008;326:196–208.

[28] Yang F, Lim GP, Begum AN, Ubeda OJ, Simmons MR, Ambegaokar SS, et al. Curcumin inhibits formation of amyloid  $\beta$  oligomers and fibrils, binds plaques, and reduces amyloid in vivo. *J Biol Chem* 2005;280:5892–901.

[29] Agrawal R, Mishra B, Tyagi E, Nath C, Shukla R. Effect of curcumin on brain insulin receptors and memory functions in STZ (ICV) induced dementia model of rat. *Pharmacol Res* 2010;61:247–52.

[30] Dairam A, Fogel R, Daya S, Limson JL. Antioxidant and iron-binding properties of curcumin, capsaicin, and S-allylcysteine reduce oxidative stress in rat brain homogenate. *J Agric Food Chem* 2008;56:3350–6.

[31] Paxinos G, Watson C. The rat brain in stereotaxic coordinates. 4th ed. London, UK: Academic Press; 1998.

[32] Maldonado PD, Molina-Jijón E, Villeda-Hernández J, Gálvan-Arzate S, Santamaría A, Pedraza-Chaverri J. NAD(P)H oxidase contributes to neurotoxicity in an excitotoxic/prooxidant model of Huntington's disease in rats: protective role of apocynin. *J Neurosci Res* 2010;88:620–9.

[33] Silva-Adaya D, Pérez-De La Cruz V, Villeda-Hernández J, Carrillo-Mora P, González-Herrera IG, García E, et al. Protective effect of L-kynurenone and probenecid on 6-hydroxydopamine-induced striatal toxicity in rats: implications of modulating kynurene as a protective strategy. *Neurotoxicol Teratol* 2011;33:303–12.

[34] Schmued LC, Hopkins KJ. Fluoro-Jade B: a high affinity fluorescent marker for the localization of neuronal degeneration. *Brain Res* 2000;874:123–30.

[35] Espada S, Ortega F, Molina-Jijón E, Rojo AI, Pérez-Sen R, Pedraza-Chaverri J, et al. The purinergic P2Y(13) receptor activates the Nrf2/HO-1 axis and protects against oxidative stress-induced neuronal death. *Free Radic Biol Med* 2010;49(3):416–26.

[36] Hamanaka RB, Chandel NS. Mitochondrial reactive oxygen species regulate cellular signaling and dictate biological outcomes. *TIBS* 2010;35:505–13.

[37] Santamaría A, Ríos C. MK-801, an N-methyl-D-aspartate receptor antagonist, blocks quinolinic acid-induced lipid peroxidation in rat corpus striatum. *Neurosci Lett* 1993;159:51–4.

[38] Aguilera P, Chávez-Cárdenas ME, Floriano-Sánchez E, Barrera D, Santamaría A, Sánchez-González DJ, et al. Time-related changes in constitutive and inducible nitric oxide synthases in the rat striatum in a model of Huntington's disease. *Neurotoxicology* 2007;28:1200–7.

[39] Maldonado PD, Chávez-Cárdenas ME, Barrera D, Villeda-Hernández J, Santamaría A, Pedraza-Chaverri J. Poly(ADP-ribose) polymerase-1 is involved in the neuronal death induced by quinolinic acid in rats. *Neurosci Lett* 2007;425:28–33.

[40] Pérez-De La Cruz V, Konigsberg M, Pedraza-Chaverri J, Herrera-Mundo N, Díaz-Muñoz M, Morán J, et al. Cytoplasmic calcium mediates oxidative damage in an excitotoxic/energetic deficit synergic model in rats. *Eur J Neurosci* 2008;27:1075–85.

[41] Sayre LM, Perry G, Smith MA. Oxidative stress and neurotoxicity. *Chem Res Toxicol* 2008;21:172–88.

[42] Dalle-Donne I, Rossi R, Giustarini D, Milzani A, Colombo R. Protein carbonyl groups as biomarkers of oxidative stress. *Clin Chim Acta* 2003;329:23–38.

[43] Norman AB, Wyatt LM, Hildebrand JP, Kolmonpumporn M, Moody CA, Lehman MN, et al. Sensitization of rotation behavior in rats with unilateral 6-hydroxydopamine or kainic acid-induced striatal lesions. *Pharmacol Biochem Behav* 1990;37:755–9.

[44] Santamaría A, Ríos C, Solís-Hernández F, Ordaz-Moreno J, González-Reynoso L, Altadrida M, et al. Systemic DL-kynurenone and probenecid pretreatment attenuates quinolinic acid-induced neurotoxicity in rats. *Neuropharmacology* 1996;35:23–8.

[45] Dong XX, Wang Y, Qin ZH. Molecular mechanisms of excitotoxicity and their relevance to pathogenesis of neurodegenerative diseases. *Acta Pharmacol Sin* 2009;30:379–87.

[46] Lee MC, Ting KK, Adams S, Brew BJ, Chung R, Guillemin GJ. Characterisation of the expression of NMDA receptors in human astrocytes. *PLoS One* 2010;5:e14123.

[47] Jellinger KA. Recent advances in our understanding of neurodegeneration. *J Neural Transm* 2009;116:1111–62.

[48] Ramsey CP, Glass CA, Montgomery MB, Lindl KA, Ritson GP, Chia LA, et al. Expression of Nrf2 in neurodegenerative diseases. *J Neuropathol Exp Neurol* 2007;66:75–85.

[49] Gao X, Dinkova-Kostova AT, Talalay P. Powerful and prolonged protection of human retinal pigment epithelial cells, keratinocytes, and mouse leukemia cells against oxidative damage: the indirect antioxidant effects of sulforaphane. *Proc Natl Acad Sci U S A* 2001;98:15221–6.

[50] Moosmann B, Behl C. Antioxidants as treatment for neurodegenerative disorders. *Expert Opin Investig Drugs* 2002;11:1407–35.

[51] Fatokun AA, Stone TW, Smith RA. Oxidative stress in neurodegeneration and available means of protection. *Front Biosci* 2008;13:3288–311.

[52] Moi P, Chan K, Asunis I, Cao A, Kan YW. Isolation of NF-E2-related factor 2 (Nrf2), a NF-E2-like basic leucine zipper transcriptional activator that binds to the tandem NF-E2/AP1 repeat of the beta-globin locus control region. *Proc Natl Acad Sci U S A* 1994;91:9926–30.

[53] Lee JM, Calkins MJ, Chan K, Kan YW, Johnson JA. Identification of the NF-E2-related factor-2-dependent genes conferring protection against oxidative stress in primary cortical astrocytes using oligonucleotide microarray analysis. *J Biol Chem* 2003;278:12029–38.

[54] Balogun E, Hoque M, Gong P, Killeen E, Green CJ, Foresti R, et al. Curcumin activates the haem oxygenase-1 gene via regulation of Nrf2 and the antioxidant responsive element. *Biochem J* 2003;371:887–95.

[55] Nishinaka T, Ichijo Y, Ito M, Kimura M, Katsuyama M, Iwata K, et al. Curcumin activates human glutathione S-transferase P1 expression through antioxidant response element. *Toxicol Lett* 2007;170:238–47.

[56] Dinkova-Kostova AT, Talalay P. Relation of structure of curcumin analogs to their potencies as inducers of Phase 2 detoxification enzymes. *Carcinogenesis* 1999;20:911–4.

[57] Hu C, Eggler AL, Mesecar AD, van Breemen RB. Modification of keap1 cysteine residues by sulforaphane. *Chem Res Toxicol* 2011;24:515–21.